This article has been accepted for inclusion in a future issue of this journal. Content is final as presented, with the exception of pagination.

freepapers.ir FREE papers

Oscillation Damping of a Distributed Generator Using a Virtual Synchronous Generator

Toshinobu Shintai, Yushi Miura, *Member, IEEE*, and Toshifumi Ise, *Member, IEEE*

***Abstract*—These days, distributed generators (DGs), such as photovoltaic, wind turbine, and gas cogeneration systems have attracted more attention than in the past. DGs are often connected to a grid by power inverters. The inverters used in DGs are generally controlled by a phase-locked loop (PLL) in order to be synchronized with the grid. In a stability point of view, the power system will be significantly affected if the capacity of inverter-based DGs becomes larger and larger. The concept of the virtual synchronous generator (VSG), which is used to control inverters to behave like a real synchronous generator, can be considered as a solution. The VSG can produce virtual inertia from energy storage during a short operation time, and the active power can be produced by a VSG similar to a synchronous generator. In this paper, an oscillation damping approach is developed for a DG using the VSG. The method is confirmed analytically, and verified through computer simulations. Finally, some laboratory experiments are conducted using 10-kW inverters and a transmission-line simulator.**

***Index Terms*—Active power control, oscillation reduction, reactive power control, swing equation, virtual synchronous generator.**

I. Introduction

THE PERCENTAGE of distributed generators (DGs) connected to the grid by inverters is in growing. For example, 14.3 GW photovoltaic is planned to be connected to the Japanese power grid by 2020 and 53 GW photovoltaic will be connected to the grid by 2030. The inverters used in DGs are generally controlled by the phase-locked Loop (PLL) in order to synchronize with the grid frequency and phase. Power systems may become unstable if the percentage of inverter type DGs becomes larger and larger, because the inverter frequency only follows the frequency determined by other synchronous generators, which is detected by PLL. If the PLL loose the locked situation by the power system disturbance, the inverter has possibility to stop the operation due to over current of ac side or over voltage of dc side, and power shortage may be occurred. However, the inverters can be controlled to behave like a synchronous generator using concept of "Virtual Synchronous Generator (VSG)" [1]. A simple VSG model is shown in Fig. 1 [1]. Using the grid voltage/frequency and state of charge (SOC) of storage device, VSG control unit sends proper control signal to the inverter in order to inject or absorb amount of power. The inverter is controlled to behave like a synchronous generator by the VSG controller. Grid stability can be improved by using the VSGs because the VSGs can provide virtual inertia similar to the rotor's inertia of synchronous generators by using energy storages, and the inverter can continue operation keeping synchronization with other generations in the power system.

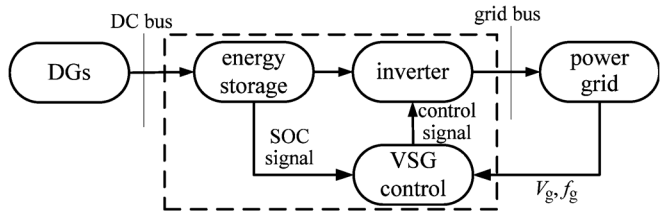

Fig. 1. VSG diagram.

There are several papers exploring the related subjects. The addressed VSGs in [2]–[5] have only an energy storage and no DGs are used. The concept of a static synchronous generator (SSG) was proposed in [6]. The control scheme of SSG is based on the Park's transformation and the swing equation. This scheme is strictly simulating characteristics of a synchronous generator. However, it is not necessary for inverters to mimic synchronous generator, perfectly. In our previous research [7], a virtual mechanical phase is established using the swing equation with simple damping term. Then it is used as a phase command of inverter output voltage. Additionally, the grid stability and VSG's response of the voltage dip were investigated. Then it was verified that VSG system enhance the grid stability. The control strategy of [8] is also established using the same equation. However, this system has to be switched to grid-connected or intentional islanding mode, appropriately. In our previous research [9], a reactive power control method was developed to keep the sending end voltage at the specified rated value and operate with the same control scheme whenever it is connected to the grid or operated in intentional islanding mode.

However, the inertia of synchronous generator may cause the oscillation of active and reactive power of the DG. The real synchronous generator mainly uses the power system stabilizer (PSS) to damp this oscillation [10]–[16]. However, it is difficult for the PSS to determine proper control parameters because the power system is an ambiguous and variable nonlinear system.

The VSG is able to cover the difficulty of determining proper control parameters. Since the VSG has no actual rotor system, one can use the swing equation via an algorithm to generate virtual inertia. However, the equation is also nonlinear and hard

Manuscript received January 23, 2013; revised March 14, 2013, June 15, 2013, and August 10, 2013; accepted September 03, 2013. Paper no. TPWRD-00107-2013.

The authors are with the Division of Electrical, Electronic and Information Engineering, Osaka University, Osaka 565-0871, Japan (e-mail: ise@eei.eng.osaka-u.ac.jp).

Color versions of one or more of the figures in this paper are available online at http://ieeexplore.ieee.org.

Digital Object Identifier 10.1109/TPWRD.2013.2281359

0885-8977 © 2014 IEEE. Personal use is permitted, but republication/redistribution requires IEEE permission.
See http://www.ieee.org/publications_standards/publications/rights/index.html for more information.

This article has been accepted for inclusion in a future issue of this journal. Content is final as presented, with the exception of pagination.

freepapers.ir FREE papers

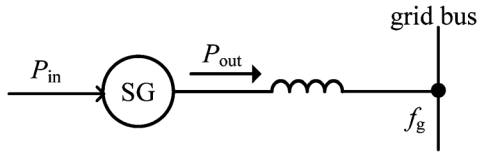

Fig. 2. Model of synchronous generator.

to determine adequate parameters. In [17], [18], linearizing technique for the power system is proposed. In this paper, a novel linearizing technique for VSG-based control scheme is proposed. Thus, the VSG can damp the grid oscillations by linear control theory. The present paper is organized as follows: an introduction on the VSG is given in Section II. Swing equation linearization and mathematical formulation are presented in Section III. Sections IV and V give simulation and experimental results, respectively. This paper is concluded in Section VI.

II. Virtual Synchronous Generator

The model of synchronous generator which is used in this paper is a cylindrical-rotor type synchronous generator (SG) connected to an infinite bus. A simplified model is shown in Fig. 2. Kinetic energy of rotor W can be expressed as follows:

$$W = \frac{1}{2} J \omega_m^2 \tag{1}$$

where J is the rotor inertia moment and ω_{m} is the rotor speed. This equation is differentiated as shown in (2); where P_{in} and P_{out} are input and output powers, respectively. Damping term $(D\Delta\omega_{\mathrm{m}})$ is also added to the equation, because the rotor of the synchronous generator has damper windings. Here, D is the damping factor and $\Delta\omega_{\mathrm{m}}$ is $\omega_{\mathrm{g}} - \omega_{\mathrm{m}}$. The ω_{g} is a rotating speed of grid voltage. The following swing equation model is used to realize the VSG structure:

$$P_{\mathrm{in}} - P_{\mathrm{out}} = J\omega_m \frac{\mathrm{d}\omega_m}{\mathrm{d}t} - D \cdot \Delta\omega_m. \tag{2}$$

The structure of the used VSG is shown in Fig. 3. The swing (2) is used to drive the power inverter. As a result, the inverter behaves as a synchronous generator. Grid frequency and output power are measured by the frequency detector and the power meter blocks, respectively. The grid frequency is used to calculate $\Delta\omega_{\mathrm{m}}$. Then, the virtual rotor speed ω_{m} is calculated by the VSG control block using (2). Runge-Kutta method is used to obtain the ω_{m}. The virtual mechanical phase θ_{m} is obtained from ω_{m}, and it is given to the inverter as a phase control command for the inverter output voltage.

As shown in Fig. 3, when the VSG inverter is connected to the infinite bus, active and reactive power (P and Q) are expressed as

$$\begin{aligned} P + jQ &= \boldsymbol{V}_{\mathrm{grid}} \boldsymbol{I}^*_{\mathrm{grid}} \\ &= \frac{V_t V_{\mathrm{grid}}}{X_L} \sin\delta + j \frac{V_t V_{\mathrm{grid}} \cos\delta - {V_{\mathrm{grid}}}^2}{X_L} \end{aligned} \tag{3}$$

where "*" of (3) represents conjugate operator, δ is the phase difference between $\boldsymbol{V}_{\mathrm{t}}$ and $\boldsymbol{V}_{\mathrm{grid}}$. The $\boldsymbol{V}_{\mathrm{t}}$ is inverter output voltage and the $\boldsymbol{V}_{\mathrm{grid}}$ is the grid voltage. By controlling the amplitude of inverter output voltage to become $V_{\mathrm{t}} \cos\delta > V_{\mathrm{grid}}$, the inverter supplies reactive power to the grid. Conversely, when $V_{\mathrm{t}} \cos\delta < V_{\mathrm{grid}}$, the inverter consumes reactive power. It can be seen that the voltage amplitude command is obtained from the PI controller using feedback of Q_{out}. The Q^* of Fig. 3 is the reactive power command.

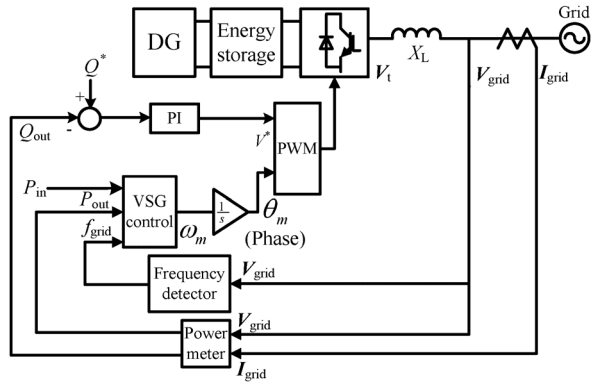

Fig. 3. VSG control block diagram.

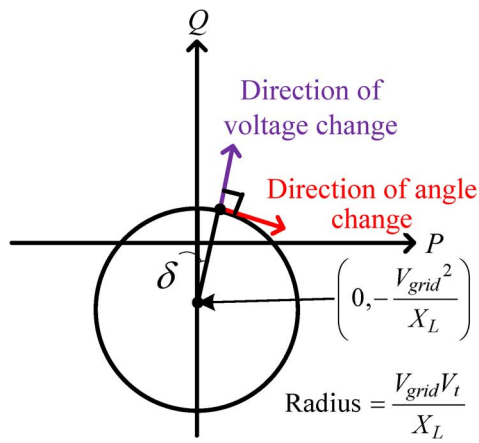

Fig. 4. Power circle diagram of (3).

III. Mathematical Formulation

A. Nonlinearity of Swing Equation

As mentioned in Section II, in a VSG, the active power P is controlled by changing δ and the reactive power Q is controlled by changing V_{t}. Normally, for a synchronous generator, it is assumed that δ is under 30 degree. In this case, $\sin\delta \cong \delta$ and $\cos\delta \cong 1$, thus the P is a function of δ and, P and Q can be independently controlled. A 2-D expression of this relationship is shown in Fig. 4.

However, if δ is over 30 degree or there is large resistance in connecting line as shown in Fig. 5, P is not only a function of δ. R and X are resistance and inductance of the line, respectively. Equation (3) can be changed to (4) and (5) in the case of existing a considerable resistance R

$$P = \frac{V_t V_{\mathrm{grid}}(R\cos\delta + X\sin\delta) - R{V_{\mathrm{grid}}}^2}{R^2 + X^2} \tag{4}$$

$$Q = \frac{V_t V_{\mathrm{grid}}(X\cos\delta - R\sin\delta) - X{V_{\mathrm{grid}}}^2}{R^2 + X^2}. \tag{5}$$

This article has been accepted for inclusion in a future issue of this journal. Content is final as presented, with the exception of pagination.

FREE papers freepapers.ir دانلود کننده مقالات علمی

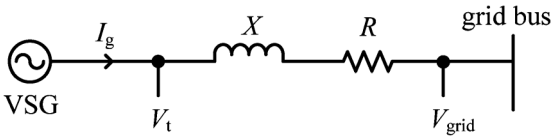

Fig. 5. Single-machine infinite bus system.

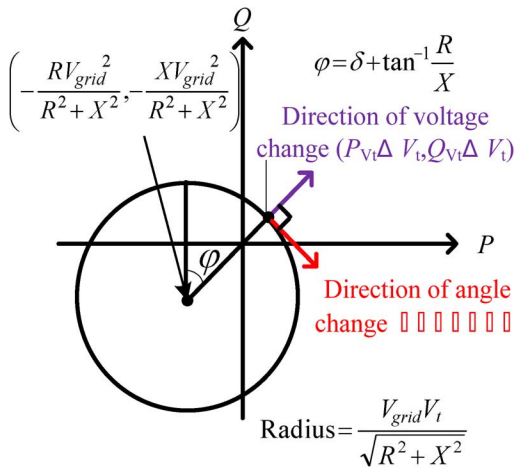

Fig. 6. Power circle diagram of (6) and (7).

Following a manipulation, (4) and (5) become (6) and (7), respectively

$$P=\frac{V_tV_{\rm grid}}{\sqrt{R^2+X^2}}\sin\left(\delta+\tan^{-1}\frac{R}{X}\right)-\frac{RV_{\rm grid}{}^2}{R^2+X^2} \quad (6)$$

$$Q=\frac{V_tV_{\rm grid}}{\sqrt{R^2+X^2}}\cos\left(\delta+\tan^{-1}\frac{R}{X}\right)-\frac{XV_{\rm grid}{}^2}{R^2+X^2}. \quad (7)$$

Thus, P contains *sine* function and makes the swing equation nonlinear. Additionally, active and reactive power controls are not independent. The two-dimensional expression of this relationship is shown in Fig. 6. The δ and $V_{\rm t}$ changes affect both P and Q. This conflict behavior makes the swing equation more complicated for realization and control.

B. Linearization and Decoupling

In order to solve the above problem, a new control equation which will not be affected by $V_{\rm t}$ is proposed. Then the equation will be linearized after detailed analysis.

By assuming P and Q as binary functions of δ and $V_{\rm t}$, total differentiation of $P(\delta,V_{\rm t})$ and $Q(\delta,V_{\rm t})$ are expressed as

$$\mathrm{d}P=P_\delta\mathrm{d}\delta+P_{Vt}\mathrm{d}V_t, \quad (8)$$

$$\mathrm{d}Q=Q_\delta\mathrm{d}\delta+Q_{Vt}\mathrm{d}V_t \quad (9)$$

where P_δ, P_{Vt}, Q_δ and Q_{Vt} are partial differential of P and Q. By setting the initial value of P and Q as P_0 and Q_0, respectively, P and Q are expressed as (10) and (11) after minor change of time Δt

$$P=P_0+\Delta P=P_0+\frac{\mathrm{d}P}{\mathrm{d}t}\Delta t$$

$$=P_0+P_\delta\frac{\mathrm{d}\delta}{\mathrm{d}t}\Delta t+P_{Vt}\frac{\mathrm{d}V_t}{\mathrm{d}t}\Delta t \quad (10)$$

$$Q=Q_0+\Delta Q=Q_0+\frac{\mathrm{d}Q}{\mathrm{d}t}\Delta t$$

$$=Q_0+Q_\delta\frac{\mathrm{d}\delta}{\mathrm{d}t}\Delta t+Q_{Vt}\frac{\mathrm{d}V_t}{\mathrm{d}t}\Delta t \quad (11)$$

where ΔP and ΔQ are minor change of P and Q, respectively. Then, $\mathrm{d}\omega_{\rm m}/\mathrm{d}t$ can be expressed as (12) by substituting (10) for $P_{\rm out}$ of (2)

$$\frac{\mathrm{d}\omega_m}{\mathrm{d}t}=\frac{(P_{\rm in}-P_0-P_\delta\Delta\delta)-P_{Vt}\Delta V_t+D(\omega_g-\omega_m)}{J\omega_m} \quad (12)$$

where $\Delta\delta$ and $\Delta V_{\rm t}$ are $(\mathrm{d}\delta/\mathrm{d}t)\Delta t$ and $(\mathrm{d}V_{\rm t}/\mathrm{d}t)\Delta t$, respectively. The term $-P_{Vt}\Delta V_{\rm t}$ shows the effect of the voltage change. If the $-P_{Vt}\Delta V_{\rm t}$ can be cancelled, the swing equation becomes no longer subjected to the voltage change

Therefore, (2) was modified by adding $m(Q^*-Q_{\rm out})$ as follows:

$$P_{\rm in}-P_{\rm out}+m(Q^*-Q_{\rm out})=J\omega_m\frac{\mathrm{d}\omega_m}{\mathrm{d}t}+D(\omega_g-\omega_m) \quad (13)$$

where

$$m=-\frac{P_{Vt}}{Q_{Vt}}. \quad (14)$$

By substituting (10) and (11) for $P_{\rm out}$ and $Q_{\rm out}$ of (13), the $\mathrm{d}\omega_{\rm m}/\mathrm{d}t$ can be expressed as

$$\frac{\mathrm{d}\omega_m}{\mathrm{d}t}=\frac{1}{J\omega_m}\{P_{\rm in}-P_0-P_\delta\Delta\delta+m(Q^*-Q_0-Q_\delta\Delta\delta)$$
$$-(P_{Vt}\Delta V_t+mQ_{Vt}\Delta V_t)+D(\omega_g-\omega_m)\}. \quad (15)$$

By substituting (14) in the term $(P_{\rm Vt}\Delta V_{\rm t}+mQV_{\rm t}\Delta V_{\rm t})$, the following equation results:

$$P_{Vt}\Delta V_t+mQ_{Vt}\Delta V_t=P_{Vt}\Delta V_t-\frac{P_{Vt}}{Q_{Vt}}Q_{Vt}\Delta V_t=0. \quad (16)$$

This means (13) is independent of the voltage change. Fig. 7 shows (16), graphically. By feed backing $P_{\rm out}+mQ_{\rm out}$, this VSG control makes it equal to $P_{\rm in}+mQ^*$. On the other hand, PI control for reactive power control makes $Q_{\rm out}$ equal to Q^*. As a result, P and Q follow their commands. In addition, $P+mQ$ axis is vertical to the radius direction. Thus the VSG control for $P+mQ$ is not subjected to the voltage deviation and is only to be controlled by the δ.

Here, m is the gradient of vector $(P_\delta\Delta\delta,Q_\delta\Delta\delta)$ in Fig. 6. The connection of P and Q is a circular form, thus change direction of P and Q which are invoked angle and voltage changes are orthogonal. Therefore, the m can be calculated as follows:

$$\frac{Q_\delta\Delta\delta}{P_\delta\Delta\delta}=-\frac{P_{Vt}\Delta V_t}{Q_{Vt}\Delta V_t}=\frac{Q_\delta}{P_\delta}=-\frac{P_{Vt}}{Q_{Vt}}=m. \quad (17)$$

When $\Delta\delta=0$ (δ is not changed), ΔP is equal to $P_{\rm Vt}\Delta V_{\rm t}$ and ΔQ is equal to $Q_{\rm Vt}\Delta V_{\rm t}$, thus, m is calculated via dividing $-\Delta P$ by ΔQ. Conversely, when $\Delta V_{\rm t}=0$ ($V_{\rm t}$ is not changed), ΔP is equal to $P_\delta\Delta\delta$ and ΔQ is equal to $Q_\delta\Delta\delta$. Thus, m is calculated via dividing ΔQ by ΔP.

This article has been accepted for inclusion in a future issue of this journal. Content is final as presented, with the exception of pagination.

freepapers.ir FREE papers دانلود کننده مقالات علمی

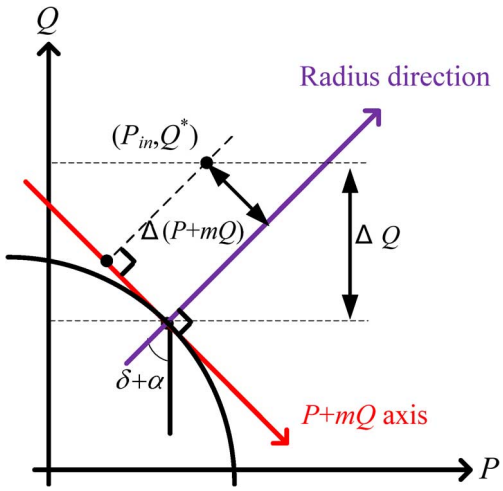

Fig. 7. Control of $P + mQ$ axis.

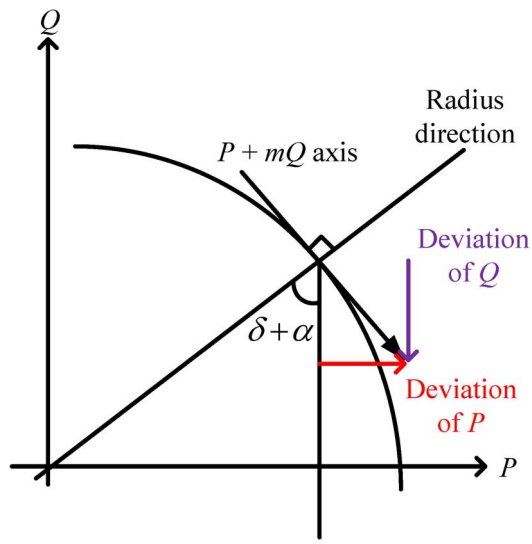

Fig. 8. $P + mQ$ deviation for P and Q.

The term of $P_{\rm in} - P_0 - P_\delta\Delta\delta + m(Q_{\rm in} - Q_0 - Q_\delta\Delta\delta)$ in (15) can be rewritten as

$$P_{\rm in} - P_0 + m(Q^* - Q_0) - \left(\frac{P_\delta^2 + Q_\delta^2}{P_\delta}\right)\Delta\delta. \tag{18}$$

Assuming P and Q as

$$P = A\sin(\delta+\alpha) - B \tag{19}$$
$$Q = A\cos(\delta+\alpha) - C \tag{20}$$

where

$$A = \frac{V_t V_{\rm grid}}{\sqrt{R^2+X^2}},\ B = \frac{R{V_{\rm grid}}^2}{R^2+X^2},$$
$$C = \frac{X{V_{\rm grid}}^2}{R^2+X^2},\ \alpha = \tan^{-1}\frac{R}{X} \tag{21}$$

and synchronizing coefficient of $P + mQ$ will be expressed as

$$\frac{P_\delta^2 + Q_\delta^2}{P_\delta} = \frac{A^2}{A\cos(\delta+\alpha)} = \frac{A}{\cos(\delta+\alpha)}. \tag{22}$$

The change of δ causes the deviation of tangent line direction as shown in Fig. 8. Thus synchronizing coefficient P_δ under $P+mQ$ control is expressed as (23), by making projection from $P + mQ$ axis to P axis

$$P_\delta = \frac{A}{\cos(\delta+\alpha)}\cos(\delta+\alpha) = A. \tag{23}$$

It is notable that the quantity of P deviation is equal to the quantity of $P + mQ$ deviation multiplied by $\cos(\delta + \alpha)$. By integrating (23), $P_{\rm out}$ is expressed as

$$P_{\rm out} = A\delta + P_0. \tag{24}$$

On the other hand, (15) can be rewritten as given in (25) by making the projection in the same way

$$\frac{{\rm d}\omega_m}{{\rm d}t} = \frac{1}{J\omega_m}\left\{P_{\rm in} - P_0 - P_\delta\Delta\delta + D(\omega_g - \omega_m)\cos(\delta+\alpha)\right\}. \tag{25}$$

The $mQ_{\rm in}$ and mQ_0 are neglected, $(P_\delta^2 + Q_\delta^2)/P_\delta$ becomes P_δ, and $D(\omega_{\rm g} - \omega_{\rm m})$ becomes $D(\omega_{\rm g} - \omega_{\rm m})\cos(\delta + \alpha)$. If D is already set to $D/\cos(\delta + \alpha)$, (25) will be changed to

$$\frac{{\rm d}\omega_m}{{\rm d}t} = \frac{1}{J\omega_m}\left\{P_{\rm in} - P_0 - P_\delta\Delta\delta + D(\omega_g - \omega_m)\right\}. \tag{26}$$

Therefore, by replacing $P_0 + P_\delta\Delta\delta$ to $P_{\rm out}$, (26) is returned to temporal differentiation form of $\omega_{\rm m}$

$$\frac{{\rm d}\omega_m}{{\rm d}t} = \frac{P_{\rm in} - P_{\rm out} + D(\omega_g - \omega_m)}{J\omega_m}. \tag{27}$$

Generally, $J\omega_{\rm m}$ can be considered as a constant at steady-state operation. Thus, in the case the deviation of $\omega_{\rm m}$ is small, (27) is able to be considered as a 2nd-order linear differential equation.

C. Applying Linear Control Theory

Given $\delta = \int(\omega_{\rm m} - \omega_{\rm g}){\rm d}t$, $\omega_{\rm g} = 2\pi f_0$, and from (24); 1st- and 2nd-order temporal differentiation of $P_{\rm out}$ are expressed as

$$\frac{{\rm d}P_{\rm out}}{{\rm d}t} = A(\omega_m - \omega_g) \tag{28}$$
$$\frac{{\rm d}^2P_{\rm out}}{{\rm d}t^2} = A\frac{{\rm d}\omega_m}{{\rm d}t}. \tag{29}$$

By substituting (28) and (29) in (27), (27) is expressed in terms of $P_{\rm out}$ as follows:

$$\frac{J_m}{A}\cdot\frac{{\rm d}^2P_{\rm out}}{{\rm d}t^2} + \frac{D}{A}\cdot\frac{{\rm d}P_{\rm out}}{{\rm d}t} + P_{\rm out} = P_{\rm in} \tag{30}$$

where $J_{\rm m}$ is a constant value that is used instead of $J\omega_{\rm m}$ under the assumption of small deviation of $\omega_{\rm m}$. Using Laplace transformation with $P_0 = 0$, (31) can be derived

$$P_{\rm out}(s) = P_{\rm in}\frac{\frac{A}{J_m}}{\left\{s^2 + \left(\frac{D}{J_m}\right)s + A/J_m\right\}s}. \tag{31}$$

This article has been accepted for inclusion in a future issue of this journal. Content is final as presented, with the exception of pagination.

دانلود کننده مقالات علمی freepapers.ir FREE papers

TABLE I
SIMULATION PARAMETERS OF THE VSG

Base Power P_{base}	1.5 MW
Base voltage V	6.6 kV
Per-unit inertia constant H	4 s
Moment of inertia J	56.3 kg・m^2
Damping factor D	0.045
Interconnecting reactance X_{L}	37% (1.5MVA base)
Interconnecting resistance R	11.4% (1.5MVA base)
PI control gain k_p	0.05
PI control time constant k_i	0.001 s

Equation (31) is the same form as the well-known response of a typical 2nd-order control system to a step input

$$Y(s) = \frac{\omega_n^2}{(s^2 + 2\zeta\omega_n s + \omega_n^2)\, s} \tag{32}$$

where ω_{n} is the undamped natural frequency, and ζ is the damping ratio of the system. The response performance of the system can be changed by changing the damping ratio. Comparing (31) to (32), the ω_{n} and ζ is expressed as (33) and (34)

$$\omega_n = \sqrt{\frac{A}{J_m}} \tag{33}$$

$$\zeta = \frac{D}{2\sqrt{AJ_m}}. \tag{34}$$

Thus, in the case of realization of

$$D = 2\zeta\sqrt{AJ_m} \tag{35}$$

it can damp the oscillation, adequately.

IV. SIMULATIONS

To verify the proposed control method, a simulation using software PSCAD/EMTDC is performed. In our previous research [7], a distributed generator which output is 6.6 kV and 1.5 MW is used to verify VSG control. Thus, the equal-sized generator is used in this session. A conventional damping control method and developed control approach based on linearization and linear control theory are shown.

A. Conventional VSG Damping Control

To affirm the difficulty of control in the case of $\sin\delta \neq \delta$, a simulation is carried out. Then the VSG is driven in grid-connected mode. The model of simulated system is shown in Fig. 9, and the simulation parameters are shown in Table I. The reactance X_{L} and resistance R include the distribution line impedance in addition to the impedance of the inter-connecting inductor of the voltage source inverter. In distribution lines, the reactance and resistance is almost the same value. The value of X_{L} includes the reactance in the inverter and transformer. The VSG control block in Fig. 9 is the same as Fig. 3. Equation (2) is used to calculate the ω_{m}. Under the condition that active power is 1.0 MW, reactive power reference is changed from 0

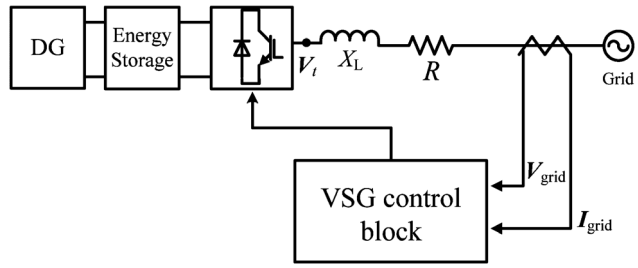

Fig. 9. Grid-connected system with resistance.

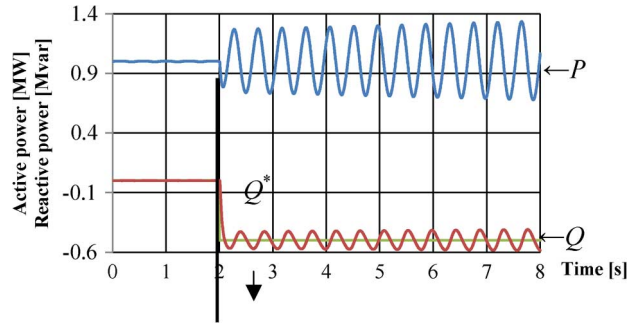

Fig. 10. Simulation results of the conventional control model.

to -0.5 Mvar at 2 s. Here, minus sign for reactive power shows the leading property. Simulation results are shown in Fig. 10.

After changing the command, an undamped oscillation appears in the system response. This phenomenon is occurred by hunting between active and reactive power controls. The V_{t} deviation cancels the damping factor in (12) under this condition. Thus, P and Q are not able to converge to the reference value.

B. Proposed Damping Control

By changing the control equation from (2)to (13), the VSG control for active power is linearized and to be independent from the voltage change. First, the gradient m should be obtained for the control equation. In this VSG control, the phase difference δ is unknown because there is no phase detection system. In addition, it is assumed that the line impedance is also unknown in this paper. Thus, the algorithm is constructed without the values of δ, R and X.

The algorithm for estimating the m value is summarized as follows.

Step 1) Set initial value of m (here, -0.1 is used as the initial). Then, go to Step 2).

Step 2) By temporal differentiating P, Q, δ and V_{t}, calculate $\mathrm{d}P/\mathrm{d}t$, $\mathrm{d}Q/\mathrm{d}t$, $\mathrm{d}\delta/\mathrm{d}t$, and $\mathrm{d}V_{\text{t}}/\mathrm{d}t$ in every iteration. Then, go to Step 3).

Step 3) Compare the temporal differential to the previous value. When the sign of $\mathrm{d}\delta/\mathrm{d}t$ is changed and $\mathrm{d}V_{\text{t}}/\mathrm{d}t$ is not changed, go to Step 4). When the sign of $\mathrm{d}V_{\text{t}}/\mathrm{d}t$ is changed and $\mathrm{d}\delta/\mathrm{d}t$ is not changed, also go to Step 4. Otherwise, go to Step 6).

Step 4) If $\mathrm{d}P/\mathrm{d}t = 0$ or $\mathrm{d}Q/\mathrm{d}t = 0$ (in steady state), m is inestimable. Thus, go to Step 6). Otherwise, go to Step 5).

This article has been accepted for inclusion in a future issue of this journal. Content is final as presented, with the exception of pagination.

دانلود کننده مقالات علمی freepapers.ir FREE papers

Step 5) Renew m. When the sign of $\mathrm{d}\delta/\mathrm{d}t$ is changed, $m = -(\mathrm{d}P/\mathrm{d}t)/(\mathrm{d}Q/\mathrm{d}t)$. When the sign of $\mathrm{d}V_\mathrm{t}/\mathrm{d}t$ is changed, $m = (\mathrm{d}Q/\mathrm{d}t)/(\mathrm{d}P/\mathrm{d}t)$. If m is plus, stop renewing m. Then, go to Step 6).

Step 6) Apply low pass filter in order to smoothing the m output. Then, go back to Step 2).

P, Q, δ and V_t are measured in each sampling time step. The m can be calculated from (17) at each iteration. Additionally, referring to (8) and (9), (36) is satisfied when $\mathrm{d}\delta/\mathrm{d}t = 0$, and (37) is satisfied when $\mathrm{d}V_\mathrm{t}/\mathrm{d}t = 0$

$$m = -\frac{P_{Vt}}{Q_{Vt}} = -\frac{\Delta P}{\Delta Q} = \frac{-\frac{\mathrm{d}P}{\mathrm{d}t}}{\frac{\mathrm{d}Q}{\mathrm{d}t}} \tag{36}$$

$$m = \frac{Q_\delta}{P_\delta} = \frac{\Delta Q}{\Delta P} = \frac{\frac{\mathrm{d}Q}{dt}}{\frac{\mathrm{d}P}{\mathrm{d}t}}. \tag{37}$$

In the VSG system, since the δ is unknown value, $(\omega_\mathrm{m} - \omega_\mathrm{g})$ is assumed as $\mathrm{d}\delta/\mathrm{d}t$. If $\mathrm{d}P/\mathrm{d}t = 0$ or $\mathrm{d}Q/\mathrm{d}t = 0$, m is inestimable. Thus, the calculation is skipped if these values are under a given threshold value. In the system of this simulation, m is always a negative value because it is assumed that the DG is a generator in this paper. Therefore, if m is positive, it is considered as a wrong value. Moreover, the m is discrete and variable because the m can only be calculated at the point that $\mathrm{d}\delta/\mathrm{d}t = 0$ or $\mathrm{d}V_\mathrm{t}/\mathrm{d}t = 0$. To smooth the behavior of m, a low pass filter is used. In addition, it is supposed that the impedance value between the inverter and the infinite bus is unknown. Therefore the m is also unknown without measurement and calculation. However, the initial value of m is necessary for proposed algorithm. Then the -0.1 is temporarily set as the initial value.

Furthermore, the damping factor D must be changed to $D/\cos(\delta + \alpha)$ as shown in (25) and (26). Thus, the calculation of damping factor $D/\cos(\delta + \alpha)$ is necessary. It can be calculated as follows (the m is equal to $-\tan(\delta + \alpha)$):

$$D' = \frac{D}{\cos(\delta + \alpha)} = D\sqrt{1 + \tan^2(\delta + \alpha)} = D\sqrt{m^2 + 1}. \tag{38}$$

To verify the proposed damping control scheme, a simulation is carried out. The condition of the simulation is the same as Section IV-A. Reactive power reference is changed from 0 to -0.5 Mvar at 2 s. By applying (13) and (38), The VSG damping control becomes independent from the voltage deviation. The threshold of $\mathrm{d}P/\mathrm{d}t$ and $\mathrm{d}Q/\mathrm{d}t$ is set at 0.02 p.u./s and the time constant of low pass filter is set at 1 s. The threshold value is determined to exclude noises of measured P and Q. If the distributed generator is steady state, $\mathrm{d}P/\mathrm{d}t$ and $\mathrm{d}Q/\mathrm{d}t$ are ideally 0. However, there must be some noises if they are measured by real system. Therefore the m cannot be converged if the threshold is too small because $\mathrm{d}P/\mathrm{d}t$ and $\mathrm{d}Q/\mathrm{d}t$ become differentiation of the noises. We found the 0.02 p.u./s by trial and error. Further discussion is needed to derive optimal threshold value. Simulation results are shown in Fig. 11.

The oscillation is effectively damped compared with Fig. 10. The $\mathrm{d}P/\mathrm{d}t$ and $\mathrm{d}Q/\mathrm{d}t$ is under the threshold at 3.5 s, the control system cease updating the m value. The m is about -0.36 at 0 s because the simulation started before 0 s and the initial value of m (-0.1) is renewed by the algorithm mentioned in above. The response of m shown in Fig. 11 is due to the low pass filter

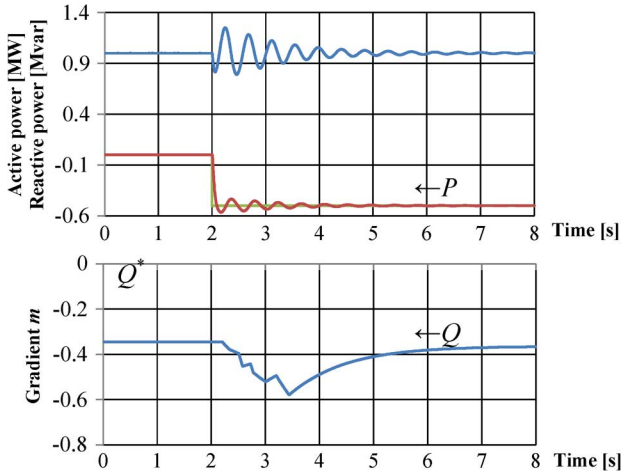

Fig. 11. System response using proposed control method.

to smooth the behavior of m. As a result, linearizing and decoupling for oscillation dumping are succeeded.

Now, the occurred oscillation is damped by the linear control theory-based approach explained in Section III-C. First, the coefficient A has to be calculated because it is assumed that the A is unknown without measurement and calculation.

The algorithm for calculating the A value is as follows.

Step 1) Set initial value of A such that the D becomes 0.045 (this is the same as conventional control mode). Then go to Step 2).

Step 2) By temporal differentiating P, δ and V_t, calculate $\mathrm{d}P/\mathrm{d}t$, $\mathrm{d}\delta/\mathrm{d}t$ and $\mathrm{d}V_\mathrm{t}/\mathrm{d}t$ in every iteration. Then go to Step 3).

Step 3) Compare the temporal differential to the previous value. When the sign of $\mathrm{d}V_\mathrm{t}/\mathrm{d}t$ is changed and $\mathrm{d}\delta/\mathrm{d}t$ is not changed, go to Step 4). Otherwise go back to Step 2).

Step 4) If $\mathrm{d}\delta/\mathrm{d}t = 0$, A is inestimable. Thus, go back to Step 2). Otherwise, A is calculated as $(\mathrm{d}P/\mathrm{d}t)/(\omega_\mathrm{m} - \omega_\mathrm{g})$ according to (28). Then, proceed to Step 5).

Step 5) Calculate the D using (35). If $D < 0.045$, reset the D at 0.045. Then, go back to Step 2).

J_m is initially set at (moment of inertia) $\times$ (rated angular speed). The calculation of Step 2 is the same as Step 2) of Section IV-B. If $\mathrm{d}\delta/\mathrm{d}t$ is under the given threshold value, the calculation is skipped in Step 4). D is compelled to be over than 0.045 in order not to increase the oscillation in Step 5). In addition, the damping factor has to be calculated as (38). Therefore, (35) can be updated as follows:

$$D' = \frac{D}{\cos(\delta + \alpha)} = 2\zeta\sqrt{AJ_m(m^2 + 1)}. \tag{39}$$

To verify the control scheme, a simulation is carried out. The condition of the simulation is the same as Section IV-B. By applying the algorithm, the oscillation is controlled by the value of ζ. The cases of $D = 0.045$ (constant), $\zeta = 0.707$ and $\zeta = 1.5$ are considered. The thresholds of $\mathrm{d}P/\mathrm{d}t$ and $\mathrm{d}\delta/\mathrm{d}t$ are set at 0.02 p.u./s and 0.02 rad/s, respectively. Under the condition that the reactive power is 0 Mvar, the active power reference (P_ref) is changed from 1 to 1.5 MW. The active power step response

This article has been accepted for inclusion in a future issue of this journal. Content is final as presented, with the exception of pagination.

freepapers.ir FREE papers دانلود کننده مقالات علمی

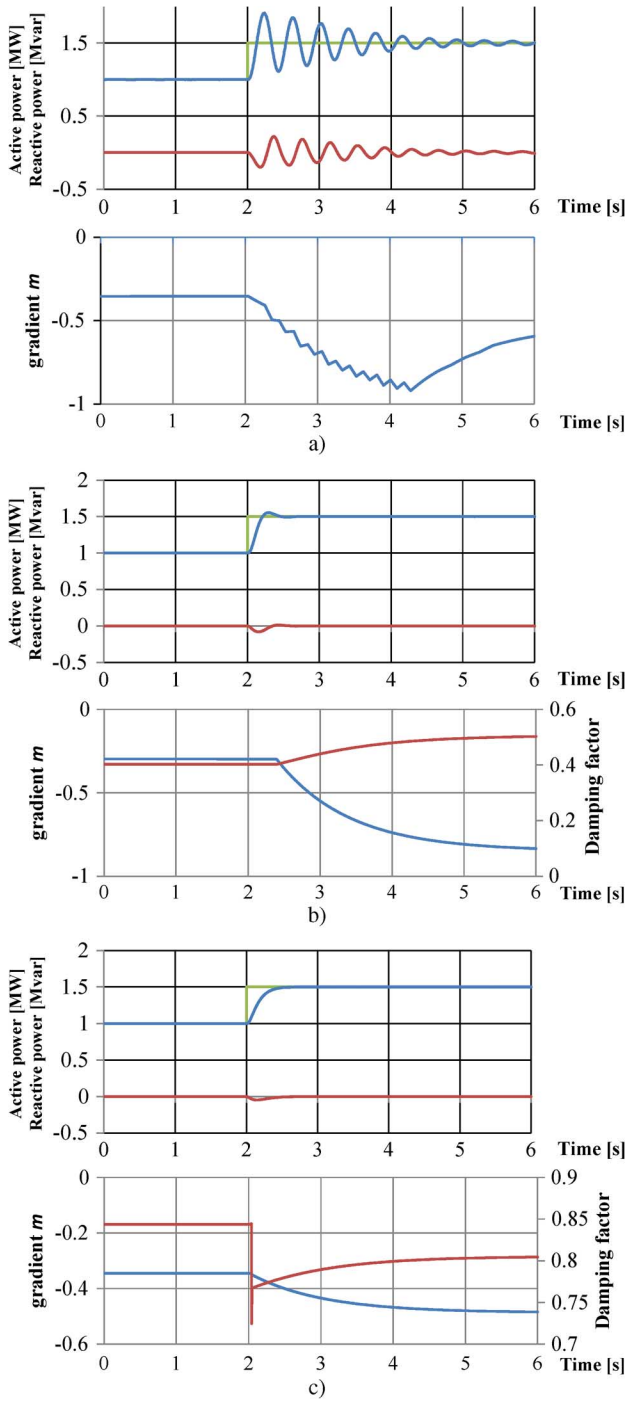

Fig. 12. System response using the proposed control method: (a) $D = 0.045$ (constant), (b) $\zeta = 0.707$, and (c) $\zeta = 1.5$.

is featured in this simulation in order to show the deference between $\zeta < 1$ and $\zeta > 1$ will be shown clearly. If $\zeta < 1$, the active power response is under damping. If $\zeta > 1$, the active power response is over damping. Simulation results are shown in Fig. 12.

In the case of constant D, the active power oscillates following changing the reference, because the VSG emulates the synchronous generator. By applying the proposed approach, the output wave form is varying along the ideal response form. In

TABLE II
SIMULATION PARAMETERS OF SG

Xd	1.90 pu	*Xq*	0.770 pu
Xd′	0.314 pu	*Xq′*	0.228 pu
Tdo′	6.55 s	*Tqo′*	0.85 s
Xd″	0.280 pu	*Xq′*	0.375 pu
Tdo″	0.039 s	*Tqo′*	0.071 s
Rated power	1 MVA	Per-unit inertia constant *H*	4 s

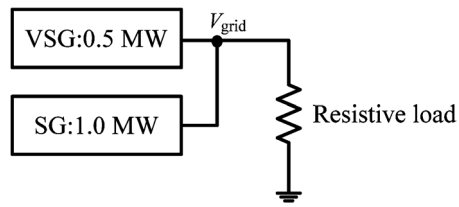

Fig. 13. Parallel running system of VSG and SG.

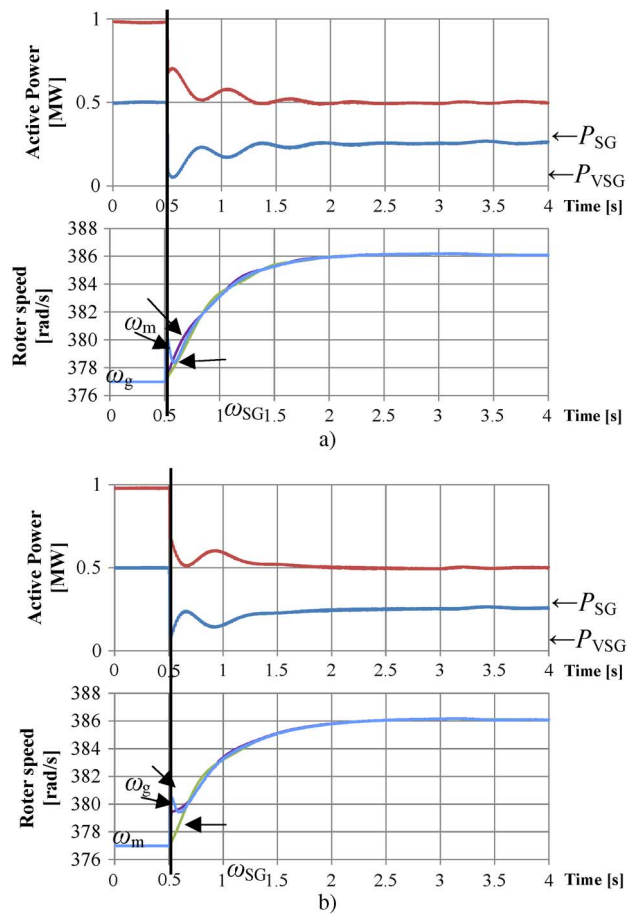

Fig. 14. Power response of VSG and SG: (a) $D = 0.045$ (constant) and (b) $\zeta = 1.5$.

the case of $\zeta = 0.707$, the response is fast with a small overshoot. On the other hand in the case of $\zeta = 1.5$, there is no overshoot but the response is slower. As a result, the oscillation is damped adequately in both cases. On the other hand, the m varies in the three cases because the changing rate of P is too small to estimate the accurate value of m. There is a trade-off

This article has been accepted for inclusion in a future issue of this journal. Content is final as presented, with the exception of pagination.

freepapers.ir FREE papers

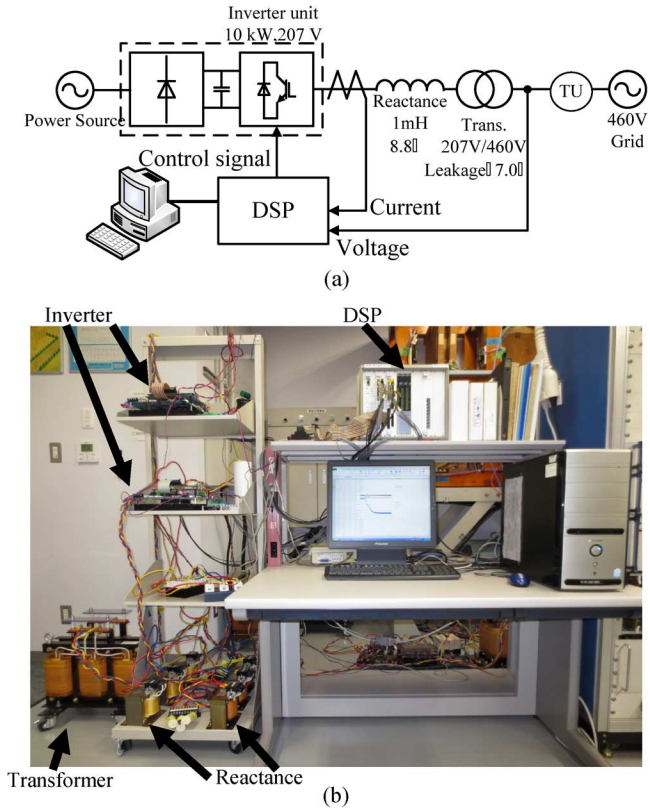

Fig. 15. Experimental system: (a) single diagram and (b) experimental facilities.

TABLE III
VSG PARAMETERS

Base power P_{base}	10 kW
Base voltage V	207 V
Per-unit inertia constant H	4 s
moment of inertia J	0.563 kg・m^2
Damping factor D	0.045
Interconnecting reactance X_{L}	15.8% (10 kVA base)
Interconnecting resistance R	2.89% (10 kVA base)
PI control gain k_p	0.0025
PI control time constant k_i	0.015 s

between estimating the accurate m and damping the oscillation. In this simulation, the oscillation damping has priority to the accurate value of m.

To verify this damping ability in intentional islanding mode, a simulation of parallel running of VSG and SG is carried out. The model of simulated system is shown in Fig. 13, and the simulation parameters of SG are shown in Table II. In addition, the VSG is applied governor control [7] for intentional islanding operation. Base power of VSG and SG are set at 0.5 MW and 1.0 MW, respectively. The damping ability is verified in the case that the load consumption is changed from 1.5 to 0.75 MW. Simulation results are shown in Fig. 14.

P_{SG} and P_{VSG} are the output active power of SG and VSG, respectively. The ω_{SG} is the rotor speed of SG. There is a cross

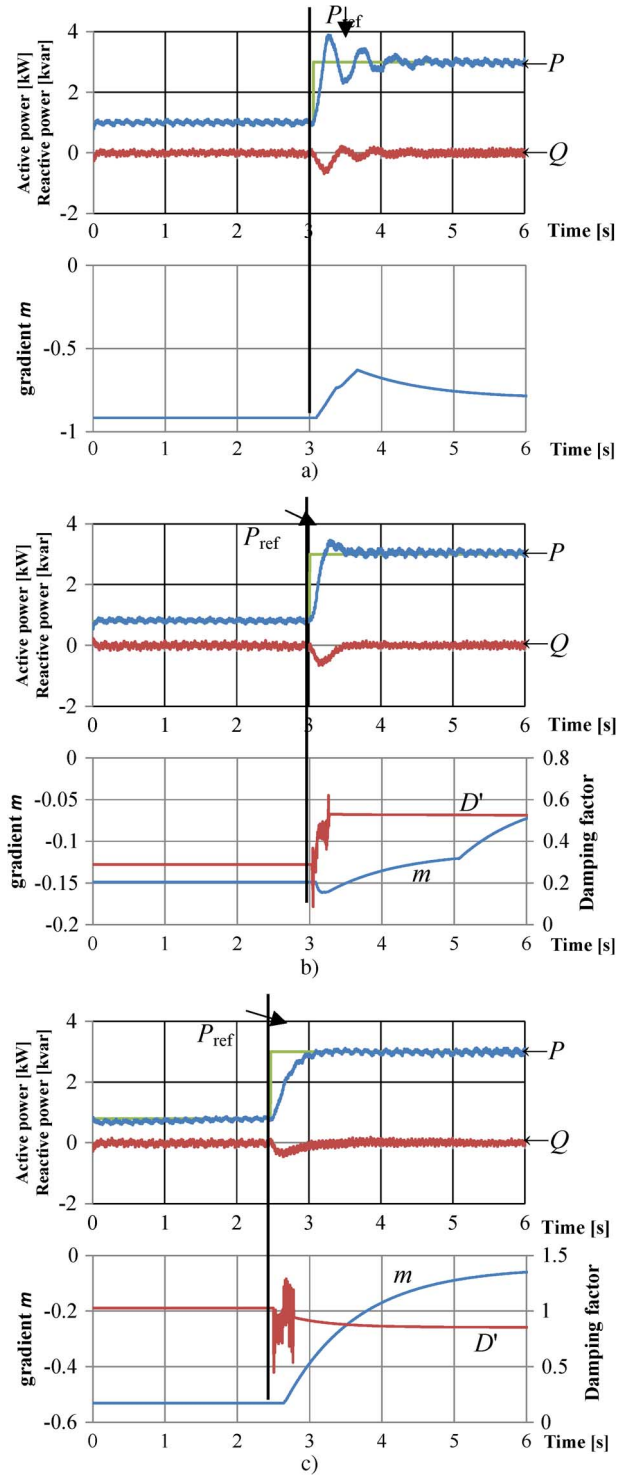

Fig. 16. Experimental results of the proposed control: (a) $D = 0.045$ (constant), (b) $\zeta = 0.707$, and (c) $\zeta = 1.5$.

current between SG and VSG in the case of a). On the other hand, the cross current is suppressed by applying the damping control as shown in Fig. 14(b). The difference of the transient response just after load changing between VSG and SG is caused due to difference of the internal reactance of VSG and SG shown in Tables I and II, respectively.

This article has been accepted for inclusion in a future issue of this journal. Content is final as presented, with the exception of pagination.

freepapers.ir FREE papers

V. Experimental Results

To show the effectiveness of the proposed control method, an experimental study for a system configuration, which is shown in Fig. 15, is carried out. A low-voltage power distribution system is considered in this session. The experimental system consists of a VSG controlled by a digital signal processor (DSP), a reactance, and transformer. Base power and voltage are 10 kW and 207 V, respectively. The transmission unit (TU) simulates a 40 km transmission line. The unit is π equivalent circuit which has 0.11 Ω resistance, 2.58 mH inductance, and 3.34 μF capacitance [7].

An experimental test scenario is conducted for the proposed control method described in Section IV-B. VSG parameters are shown in Table III. The interconnecting reactance X_{L} in the table is the total of the reactance (8.8%) and leakage reactance of the transformer (7.0%) shown in Fig. 15 (a). When the reactive power keeps 0 kvar, the active power command is changed from 1 to 3 kW. The thresholds for m and A are set at 0.6 p.u./s and 0.1 rad/s, respectively. These values have to be larger than the simulation's because there are more noises in the measured values, especially for derivatives of P and Q in (36) and (37). Thus, these values were determined by trial and error again. The cases of $D = 0.045$ (constant), $\zeta = 0.707$ and $\zeta = 1.5$ are considered. The experimental results are shown in Fig. 16.

By applying the proposed damping method, the oscillation by emulating synchronous generator is significantly damped. The response of the case $\zeta = 0.707$ has an overshoot similar to the simulation result. However, the response is quicker than that of $\zeta = 1.5$.

VI. Conclusion

To resolve the problem of power grid instability in the presence of a high percentage of inverter-based DGs, the VSG which is the concept of controlling an inverter to behave like a synchronous generator is studied. A novel control system for VSG which solves the output power oscillation occurred by the characteristic of the simulated synchronous generator is proposed. By linearizing the system equation and decoupling the voltage deviation and damping factor, and using a linear control theory, a new damping control approach is proposed. Using the developed method, the VSG evades the unstable low-frequency oscillation mode. Simulations and experimental results show that the proposed method damps the oscillation adequately.

References

[1] J. Driesen and K. Visscher, "Virtual synchronous generators," in *Proc. IEEE Power Energy Soc. Gen. Meeting—Convers. Del. Elect. Energy 21st Century*, 2008, pp. 1–3.

[2] N. Zhi, Z. Hui, and J. Liu, "Overview of microgrid management and control," in *Proc. Int. Conf. Elect. Control Eng.*, 2011, pp. 4598–4601.

[3] M. P. N. van Wesenbeeck, S. W. H. de Haan, P. Varela, and K. Visscher, "Grid tied converter with virtual kinetic storage," *Proc. IEEE Powertech Conf.*, pp. 1–7.

[4] M. Torres and L. A. C. Lopes, "Virtual synchronous generator control in autonomous wind-diesel power systems," in *Proc. IEEE Elect. Power Energy Conf.*, 2009, pp. 1–6.

[5] V. Karapanos, S. de Haan, and K. Zwetsloot, "Real time simulation of a power system with VSG hardware in the loop," in *Proc. 37th Annu. Conf. IEEE Ind. Electron. Soc.*, pp. 3748–3754.

[6] Q.-C. Zhong and G. Weiss, "Static synchronous generators for distributed generation and renewable energy," in *Proc. IEEE/Power Energy Soc. Power Syst. Conf. Expo.*, 2009, pp. 1–6.

[7] K. Sakimoto, Y. Miura, and T. Ise, "Stabilization of a power system with a distributed generators by a virtual synchronous generator function," in *Proc. 8th IEEE Int. Conf. Power Electron.—ECCE Asia*, 2011, pp. 1498–1505.

[8] Y. Xiang-Zhen, S. Jian-Hui, D. Ming, L. Jin-Wei, and D. Yan, "Control strategy for virtual synchronous generator in microgrid," in *Proc. 4th Int. Conf. Elect. Utility Dereg. Restruct. Power Technol.*, 2011, pp. 1633–1637.

[9] T. Shintai, Y. Miura, and T. Ise, "Reactive power control for load sharing with virtual synchronous generator control," in *Proc. 7th Int. Power Electron. Motion Control Conf.* , pp. 846–853.

[10] A. Murdoch, S. Venkataraman, J. J. Sanchez-Gasca, and R. A. Lawson, "Practical application considerations for power system stabilizer (pss) controls," in *Proc. IEEE Power Eng. Soc. Summer Meeting*, pp. 83–87.

[11] E. Zhou, O. P. Malik, and G. S. Hope, "Design stabilizer for a multimachine power system based on the sensitivity of PSS effect," *IEEE Trans. Energy Convers.*, vol. 7, no. 3, pp. 606–613, Sep. 1992.

[12] Y. Sudou, A. Takeuchi, M. Kawasaki, Y. Mitani, M. Andou, K. Hirayama, Y. Uemura, N. Fukushima, and T. Sogabe, "Development of a parallel PSS for inter-area mode power oscillation damping," in *Proc. IEEE Power Eng. Soc. Meeting*, Jul. 18–22, 1999, vol. 1, pp. 76–82.

[13] T. Hiyama, S. Oniki, and H. Nagashima, "Evaluation of advanced fuzzy logic PSS on analog network simulator and actual installation on hydro generators," *IEEE Trans. Energy Convers.*, pp. 125–131, Mar. 1996.

[14] K. Yoshimura and N. Uchida, "Multi input PSS optimization method for practical use by considering several operating conditions," in *Proc. IEEE Power Eng. Soc. Winter Meeting*, 1999, pp. 749–754.

[15] K. Yoshimura and N. Uchida, "Proposal of remote signal input PSS for improving power transfer capability considering damping and synchronizing toruque," in *Proc. IEEE Power Eng. Soc. Winter Meeting*, 2001, vol. 3, pp. 1329–1334.

[16] A. Gholipour, H. Lesani, and M. K. Zadeh, "Performance of a ANFIS based PSS with tie line active power deviation feedback," in *Proc. 2nd Int. Conf. Power Electron. Intell. Transport. Syst.*, Dec. 19–20, 2009, pp. 267–273.

[17] Z. Jiang and L. Xiang, "Review of exact linerization method applied to power electronics system," in *Proc. Power Energy Eng. Conf.*, Mar. 27–29, 2012, pp. 1–4.

[18] G. D. Marques and P. Verdelho, "Control of an active power filter based on input-output linearization," in *Proc. 24th Annu. Conf. IEEE Ind. Electron. Soc.*, vol. 1, pp. 456–461.

Toshinobu Shintai received his the B.Sc. degree in electrical engineering from Osaka University, Osaka, Japan, in 2011, where he is currently pursuing the M.Sc. degree in electronic and information engineering.

His current research interests are inverter control for distributed generator and virtual synchronous generator for the distributed generator.

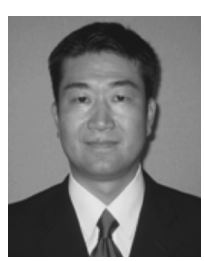

Yushi Miura (M'06) received the Ph.D. degree in electrical and electronic engineering from Tokyo Institute of Technology, Tokyo, Japan, in 1995.

From 1995 to 2004, he joined the Japan Atomic Energy Research Institute as a Researcher and developed power supplies and superconducting coils for nuclear fusion reactors. Since 2004, he has been the Associate Professor of the Division of Electrical, Electronic and Information Engineering, Osaka University. His areas of research involve power electronics, distributed generation, and superconducting technology.

This article has been accepted for inclusion in a future issue of this journal. Content is final as presented, with the exception of pagination.

freepapers.ir FREE papers دانلود کننده مقالات علمی

Toshifumi Ise (M'88) was born in 1957. He received the Ba.Sc., M.Sc., and Dr.Eng. degrees in electrical engineering from Osaka University, Osaka, Japan, in 1980, 1982 and 1986, respectively.

Currently, he is a Professor with the Division of Electrical, Electronic and Information Engineering, Graduate School of Engineering, Osaka University, where he has been since 1990. From 1986 to 1990, he was with the Nara National College of Technology, Nara, Japan. His research interests are in the areas of power electronics and applied superconductivity, including superconducting magnetic energy storage (SMES) and new distribution systems.

Prof. Ise is a Fellow of the Institute of Electrical Engineers of Japan.